HHS Public Access

Author manuscript

Exp Eye Res. Author manuscript; available in PMC 2018 July 01.

Published in final edited form as:

Exp Eye Res. 2017 July ; 160: 106–115. doi:10.1016/j.exer.2017.04.003.

A mouse ocular explant model that enables the study of living optic nerve head events after acute and chronic intraocular pressure elevation: focusing on retinal ganglion cell axons and mitochondria

Elizabeth C. Kimball[1], **Mary E. Pease**[1], **Matthew R. Steinhart**[1], **Ericka N. Oglesby**[1], **Ian Pitha**, **Cathy Nguyen**[1], and **Harry A. Quigley**[1]

[1]From the Glaucoma Center of Excellence, Wilmer Ophthalmological Institute, Johns Hopkins University, Baltimore, Maryland, USA

Abstract

We developed an explant model of the mouse eye and optic nerve that facilitates the study of retinal ganglion cell axons and mitochondria in the living optic nerve head (ONH) in an *ex vivo* environment. Two transgenic mouse strains were used, one expressing yellow fluorescent protein in selected axons and a second strain expressing cyan fluorescent protein in all mitochondria. We viewed an explanted mouse eye and optic nerve by laser scanning microscopy at and behind the ONH, the site of glaucoma injury. Explants from previously untreated mice were studied with the intraocular pressure (IOP) set artificially at normal or elevated levels for several hours. Explants were also studied from eyes that had undergone chronic IOP elevation from 14 hours to 6 weeks prior to *ex vivo* study. Image analysis in static images and video of individual mitochondria or axonal structure determined effects of acute and chronic IOP elevation. At normal IOP, fluorescent axonal structure was stable for up to 3 hours under *ex vivo* conditions. After chronic IOP elevation, axonal integrity index values indicated fragmentation of axon structure in the ONH. In mice with fluorescent mitochondria, the normal density decreased with distance behind the ONH by 45% (p=0.002, t-test). Density increased with prior chronic IOP elevation to 21,300 ± 4,176 mitochondria/mm^2 compared to control 16,110 ± 3159 mitochondria/mm^2 (p=0.025, t-test), but did not increase significantly after 4 hours, acute IOP elevation (1.5% decrease in density, p=0.83, t-test). Mean normal mitochondrial length of 2.3 ± 1.4 μm became 13% smaller after 4 hours of IOP elevation *ex vivo* compared to baseline (p=0.015, t-test, N-10). Normal mitochondrial speed of movement was significantly slower in the anterograde direction (towards the brain) than retrograde, but there were more mitochondria in motion and traveling longer lengths in anterograde direction. The percent of mitochondria in motion decreased by >50% with acute IOP increase to 30 mm Hg after 60 minutes. A new ocular explant model implemented with eyes from transgenic mice with fluorescent cellular components provided real time measurement of the early

Correspondence: Elizabeth C. Kimball, Smith Building M002, Wilmer Eye Institute, Johns Hopkins University, 400 North Broadway, Baltimore, MD USA 21287; telephone: +1 410 955 3337; fax: +1 443 287 2711; fcone1@jhmi.edu.

events in experimental glaucoma and quantitative outcomes for neuroprotection therapy experiments.

Keywords

glaucoma; sclera; mouse; retinal ganglion cell; axons; mitochondria; transport block

1. Introduction

Glaucoma is the most common preventable cause of blindness worldwide (Quigley and Broman, 2006), and its damaging effects are known to be mediated through alterations at the optic nerve head (ONH) and degradation of the retinal ganglion cells (RGC), produced by the action of intraocular pressure (IOP) (Anderson and Hendrickson, 1974; Quigley et al., 1981). In mouse glaucoma, axonal abnormality is first detected in the unmyelinated axon segment at and just behind the ONH (Howell et al., 2007). Consequently, the study of RGC axons and astrocytes is highly relevant to glaucoma damage mechanisms. Several genetically modified mouse lines with fluorescent axons or astrocytes permit the study of internal axonal and astrocytic behavior not yet possible in other animal models.

Two transgenic mouse strains were used for this study. The first expresses yellow fluorescent protein (YFP) in a small number of RGCs. Previously, we and others (Danaf and Huberman, 2015; Johnson et al., 2016; Kalesnykas et al., 2012; Leung et al., 2011) have studied changes in RGC bodies and dendrites of the RGC-YFP strain with chronic IOP elevation. Some investigations were performed by cross-sectional study in histological preparations, while others observed sequential events in these cells by ophthalmoscopy. There was no existing method permitting observation of the axonal events in living neural tissue at the ONH, a major site of injury, after exposure to IOP elevation. We developed the present explant model to view events at this site during acute elevations in IOP in both normal and chronic glaucoma mouse eyes. To move beyond studying axonal structure, we used the same explant model in eyes and optic nerves (ON) from a second strain of mice expressing cyan fluorescent protein (CFP) in all mitochondria.

Energy provided to axons and glia in the ONH comes from adenosine triphosphate (ATP), largely generated within mitochondria. In RGCs, there is bidirectional, intra-axonal transport of mitochondria (Kang et al., 2008; Miller and Sheetz, 2006; Sheng and Cai, 2012). Mitochondria with high ATP levels travel anterograde (towards the brain), while those that are energy-depleted move preferentially back toward the cell body are moving retrograde (Miller and Sheetz, 2004). Mitochondrial density is normally higher within the ONH than elsewhere in RGC (Barron et al., 2004), and their density increases at the ONH due to axonal transport blockage in human glaucoma eyes (Quigley et al., 1981) and in experimental animal glaucoma (Minckler et al., 1978). In cultured neurons, hydrostatic pressure increase causes fission of mitochondria and loss of cellular ATP (Ju et al., 2007). The number of mitochondria in DBA/2J glaucoma mouse optic nerve was increased and their surface area decreased by histological study (Coughlin et al., 2015). If the energy-requiring processes of axons are affected by acute or chronic IOP elevation, such nutritional

failure may be a primary pathological event (Tezel, 2011; Osborne, 2010; McElnea et al., 2011). This hypothesis is supported by studies showing beneficial effects of free radical mitigation in experimental glaucoma (Dai et al., 2011; Inman et al., 2013; Kim et al., 2015; Lee et al., 2014). In cultured neurons, higher tensile strains slow axonal transport, a known feature of glaucoma. In cultured neurons and tissue explants, three-fourths of axonal mitochondria are stationary at a given time (Sheng and Cai, 2012; Misgeld et al., 2007). The remaining mitochondria are mobile, two thirds moving anterograde and the remaining third moving retrograde.

The explanted eye with attached optic nerve was used here for the first time to study the events occurring within the axon under conditions of controlled IOP by laser scanning microscopy. Acute IOP elevations were performed in mouse eyes with and without prior chronic IOP exposure to study the earliest intra-axonal events of glaucoma in real time.

2. Methods

2. 1. Animals

All animals were treated in accordance with the ARVO Statement for the Use of Animals in Ophthalmic and Vision Research, using protocols approved and monitored by the Johns Hopkins University School of Medicine Animal Care and Use Committee. Two transgenic mouse strains were used, one expressing YFP in selected axons (B6.Cg-Tg(Thy-1YFP)HJrs/J, Jackson Catalog Number 3782, RGC-YFP) and a second expressing CFP in all mitochondria (B6.Cg-Tg(Thy-1CFP/COX8A)S2Lich/J, Jackson Catalog Number 7967, Mito-CFP); both were obtained from Jackson Laboratories, Bar Harbor, ME. These transgenic mice express YFP and CFP under the control of the mouse thymus cell antigen 1, theta (Thy1) promoter. YFP is specifically localized to the motor, sensory and central neurons, including a small number of RGCs. CFP is expressed in mitochondria of many cell types by a human cytochrome c oxidase, subunit 8A (ubiquitous), targeting signal fused to the N-terminus. The RGC-YFP and Mito-CFP animals are bred on a C57BL/6 background. We studied a total of 64 animals under 6 months of age (see Table 1 for detailed description of each experimental study and animal number).

2.2. Chronic IOP Elevation Model

Mice were anesthetized with an intraperitoneal mixture of ketamine (Fort Dodge Animal Health, Fort Dodge, IA), xylazine (VedCo Inc., Saint Joseph, MO) and acepromazine (Phoenix Pharmaceuticals, Burlingame, CA)(50, 10 and 2 mg/kg, respectively). One anterior chamber was injected with Polybead Microspheres (Polysciences, Inc., Warrington, PA, USA), consisting of 2 μL of 6 μm diameter beads, then 2 μL of 1 μm diameter beads, followed by 1 μL of viscoelastic compound (10 mg/ml sodium hyaluronate, Healon; Advanced Medical Optics Inc., Santa Ana, CA). The injections were made through a glass cannula with a 50 μm tip diameter, connected to a Hamilton syringe (Hamilton, Inc., Reno, NV). The contralateral eye was used as control. Among the 25 RGC-YFP mice studied, there were 3 eyes used as control explants and 25 eyes explanted after chronic glaucoma. Tissue was explanted at one of 4 time points post glaucoma induction; 14 hours (N=6), 1 day (N=5), 4 days (N=7), or 7 days (N=7).

There were a total of 12 Mito-CFP animals studied; 8 received the glaucoma bead model injection and 4 were naïve controls (both eyes from these animals were tested as controls, along with 6 contralateral eyes from the glaucoma treated group, for a total of 14 explants).

2.3. Specimen Preparation for Explant Imaging

Mice were deeply anesthetized by injection of intraperitoneal anesthetic mixture. IOP measurements were taken with a Tonolab Tonometer (TioLat, Inc., Helsinki, Finland) and eyes with attached optic nerves were enucleated and the animals were euthanized. A cautery mark on the superior cornea provided subsequent orientation. In initial experiments, eyes of each animal were kept in chilled Neurobasal Solution (NB, Thermo Fisher Scientific, Waltham, MA) for cleaning of extraocular tissue and for pre-imaging storage. We determined that this cold period did not alter any key parameters of interest and subsequent studies were done at room temperature throughout. Axial length and width measurements were taken using a digital caliper (Instant Read-Out Digital Caliper; Electron Microscopy Sciences, Hatfield, PA, USA). Each eye was glued using slow drying cyanoacrylate with the superior side facing up onto a pre-made plastic chuck (Figure 1A). Special care was taken to ensure that the nerve was flat on the chuck surface and glue did not overlie the optic nerve zone. Eight μL of 1% agarose (Sigma A4603, St. Louis, MO) pre-heated to 37°C was applied to the optic nerve. A paint brush was used to ensure the optic nerve lay flat on the chuck surface as the agarose solidified. The agarose minimized tissue motion. For the acute inflation tested samples, the anterior chamber of the eye was cannulated with a 30 gauge needle that was connected to a reservoir of NB whose height determined IOP. The baseline IOP was set to 10 mm Hg and the specimen was imaged after one minute. The mouse sclera was not always fully inflated at IOP less than 10 mm Hg.

2.4. Image Collection

Imaging was performed on a Zeiss 710 Confocal Laser Scanning Microscope (LSM 710, Carl-Zeiss, Oberkochen, Germany) in two- photon laser (2P) (Chameleon Ultra II, Coherent Inc, Santa Clara, CA), using an objective inverter arm with one of two dipping lenses: 20× or 40× W Plan-Apochromat VIS IR series, each with 1.0 NA (Carl-Zeiss, Oberkochen, Germany). Once the eye was securely glued and ON covered in agarose, NB was added and the eye and nerve were positioned underneath the inverter and the 20× lens for RGC-YFP explants and 40× lens for Mito-CFP explants. In the RGC-YFP explants. For the RGC-YFP explants, the 2P laser for LSM imaging was set at 950 nm excitation and the output (pseudo-color yellow; Figure 1B) collected using a 500-550 band pass filter. A set of images was taken at the ONH as close to the eye as possible, then sequentially along the nerve away from the eye every 425 μm. At each location, a series of 2-dimensional images was obtained in 1 μm intervals to a depth of 75-100 μm (z-stack). Two types of images were obtained, either a full frame image (425 × 425 μm) or a smaller region of interest (425 μm × 100 μm).

In the Mito-CFP explants, the excitation wavelength was 850 nm for mitochondria (pseudo-color blue, and a band-pass filter allowing 500-550 nm for second harmonic generation imaging to demonstrate collagen fibers (pseudo-color red; Figure 1C). The collagen imaging was used to identify the position of the tissues and ONH. A set of images was obtained as close to the ONH as possible, proximal to the globe, with a time series of 2-dimensional

slices at depths up to 60 μm. In control and glaucoma tissue, additional image sets were taken every 200 μm in a distal direction, moving away from the eye, toward the optic nerve cut end, up to 1.5 mm behind the globe. For measurement of mitochondrial movement, a particular position was reimaged 30 times, every 4 seconds for a total of 2 minutes. When studying speed of mitochondria, images were only taken as close to the ONH in every specimen, and more than one area was studied in select specimens. Due to potential bleaching effect of the laser excitation, when multiple images of the same nerve were performed, we imaged at different depths in the ONH.

2.5. Acute Pressure Elevation

Some normal, explanted YFP-RGC and Mito-CFP eyes underwent acute IOP elevation in the imaging apparatus under observation. After allowing the IOP to equilibrate for 10 minutes, the reservoir was raised to 30 mmHg, and images were collected 1 minute, 10 minutes, 1 hour, 2 hours, 3 hours and 4 hours after pressure elevation. Due to motion of the explant, or time constraints, 4 hour images were not obtained on all specimens. After IOP elevation, IOP was returned to 10 mm Hg for 10 minutes, one final image set was obtained. A total of 11 Mito-CFP mice were studied; 6 mice had explants studied from both left and right eyes, with IOP acutely elevated for 3 hours, but one explant was eliminated due to poor cannulation, totaling 11. In the remaining 5 mice, all eyes was studied with IOP elevation for 4 hours, totaling 10 explant samples. YFP-RGC explants five were studied; three were cannulated to baseline pressure set and kept to 10 mm Hg, while the remaining two were studied after elevation to 50 mm Hg for 3 hours.

2.6. Axon Integrity

With glaucoma injury, it was expected that axon swelling and fragmentation would occur. To measure the degree of degeneration in the RGC-YFP explants, the axonal integrity ratio (Knöferle et al., 2010) was used. Each RGC-YFP ONH Z stack was converted into a maximum projection image, allowing all axons from the 70-100 micron volume to appear within a single 2 dimensional image. Axons that were located within the projection image were identified and marked for subsequent quantification with Zen Blue software (Carl-Zeiss, Oberkochen, Germany). The measurement tool in Zen Blue was used to measure each axon's total length. In axons that exhibited gaps in the fluorescence, the length of each fragment (from gap to gap) was also measured to derive the number of fragments, the mean fragment length and the total fragment length. The parameter called axon integrity was then calculated by dividing the fragment total length by the total axon length.

2.7. Mitochondrial Speed and Distance Moved Quantification

Using a specific imaging protocol, we measured mitochondrial speed by acquiring images at the same position every 4 seconds for 2 minutes (30 images total). All moving mitochondria that were visible in successive images were measured using the distance tool of the Zeiss Zen software package. Each mitochondrion was marked in the first image of the time-series where it was visibly mobile, then it was marked in each image through the stack until it appeared motionless. Nearly all mitochondria movement was in the y-direction (along the axon). Mitochondria that moved in tight circular, repeating patterns were not counted, since they were assumed to be within glial or vascular cells, not axons. The speed was calculated

by dividing the total distance of movement from the initial to final position by the time elapsed between the images.

2.8. Mitochondrial Density and Size Quantification

To estimate mitochondrial density and mean individual mitochondrion size, images were converted to an 8bit, grey scale, 200 μm by 100 μm image window using Photoshop. Using Metamorph Imaging Analysis software, the following parameters were collected: total number of mitochondria per field, minimum diameter (the smallest diameter of each mitochondrion), maximum diameter (the greatest diameter of each mitochondrion), average diameter (average of 20 measurements from center point to exterior edge of each mitochondrion), mitochondrion area (using average diameter calculation), and total area (area of all mitochondria per field). The density of mitochondria was the total number of mitochondria divided by the area of the field of view.

2.9. Statistical Analysis

Data were tabulated and compared in RGC-YFP explants for axon integrity index between controls, acute IOP elevation and chronic IOP elevation (glaucoma) groups. Likewise, within each of the Mito-CFP explants, comparisons were made between control and prior glaucoma treated eyes, and between normal eyes at baseline versus acute IOP elevation to 30 mm Hg for various times. T-tests or non-parametric Mann Whitney tests were used to estimate statistical significance of results for axon and mitochondrial parameters.

3. Results

3.1. Imaging Stability

To show that axons and mitochondria retained their baseline structure and function during the period of 3-4 hours from explantation through the end of imaging studies, we examined images taken hourly. RGC-YFP axons showed stability up for 3 hours after baseline images were acquired, with no change in the apparent thickness of the axon and no substantial change in the brightness of fluorescence (Figure 2). Mito-CFP explants had no statistical variation in the number of mitochondria ($p=0.97$, t-test) or in diameter ($p=0.89$, t-test) from initial measurements to 3 hours later (N= 4 explants). We found that mitochondrial speed measurements with significantly more images or shorter intervals between images led to bleaching effects. To prevent signal degradation, imaging location in the z plane was changed by 2 μm at each time point.

3.2. Axon Integrity

In RGC-YFP explants that were exposed to acute IOP elevation without prior IOP elevation, there were no detectable changes from baseline in axon integrity (a normal value is an index = 1). The median axon integrity ratio remained at 1.0 after IOP elevation to 50 mm Hg for 3 hours. With chronic IOP elevation for 14 hours or longer prior to explantation and study, the integrity index declined and progressively worsening in specimens at 1, 4 and 7 days after IOP elevation ($p = 0.035$, linear regression; Table 2). The progressive fragmentation of axons after chronically elevated IOP was evident and tended to occur in the area closer to the eye (Figure 3).

3.3. Mitochondrial Density and Size

The density in the immediate ONH area was 16,110 ± 3159 mitochondria /mm^2 in control nerves immediately adjacent to the eye, with a decline in the two most distal segments that were studied (Table 3). Estimates of the number of mitochondria indicated approximately 32 mitochondria in each 1 mm length of an axon. With acute IOP elevation to 30 mm Hg for 4 hours, the density of mitochondria did not change significantly during the 4 hours of elevation. After 3 days of chronic IOP elevation, the total area of mitochondria increased by as much as 73% in areas at and behind the ONH (Table 3). Likewise, the density was increased to 21,300 ± 4,176 mitochondria /mm^2 at the ONH after 3 days of chronic IOP elevation (bead model; Table 3, Figure 4). The overall density increase was accompanied by local accumulations of mitochondria visible in laser scanning images (Figure 4), likely corresponding to the expanded axonal fragment areas seen in the YFP-RGC specimens after days of chronic IOP elevation.

The mean diameter of mitochondria in control tissues was 1.5 + 1.1 μm (N = 322 mitochondria in 10 explants, Table 3). The control mean diameter fell from 1.5 ± 1.1 μm near the nerve head to 1.1 ± 0.8 μm and 1.2 ± 0.9 μm in the two distal nerve segments, a reduction of more than 40% in total area ($p = 0.01$, mean difference at 4th segment from ONH value; linear regression for trend $r^2 = 0.73$, N = 10 control and 4 chronic glaucoma explants). With acute IOP elevation in 21 normal eye explants, mitochondrial total area and mean diameter each fell, the latter significantly at 3 and 4 hours at IOP 30 mm Hg compared to control 10 mm Hg (Table 5). The total area and diameter recovered only modestly after 10 minutes of return to 10 mm Hg. The trend for decrease in total area during acute IOP elevation was significant ($p = 0.01$, $r^2 = 0.83$, linear regression; N = 10 explants).

With 3 day chronic IOP elevation, the mean diameter was somewhat, but not significantly different from control and the trend for smaller mitochondrial size in zones further from the ONH was preserved (Table 4).

3.4. Mitochondrial Speed and Distance of Movement

The speed of mitochondrial movement and the distance traveled during a movement were studied in 4 control and 4 chronic glaucoma explants, and in 10 acute IOP elevation explants (30 mm Hg for 60 minutes). At baseline 10 mm Hg in control eyes, retrograde mean speed was 2 to 2.5 times faster than anterograde speed ($p = 0.001$, t test, Table 6). In both the anterograde and retrograde directions, the mean speed increased by a factor of 2 after 10 minutes in the explant setting compared to the first minute ($p = 0.008$, 0.02, respectively). However, at baseline, anterogradely moving mitochondria had 10% longer distance with each movement compared to retrogradely moving ones ($p = 0.05$). In the control explants of the acute IOP elevation series (N = 10), the proportion of mitochondria that were moving at any given time were 5.4% of the total in the anterograde direction and 1.8% of all mitochondria in the retrograde direction, a difference that was preserved throughout the acute IOP series data ($p = 0.01$, Table 6, Figure 5).

In the 4 explants from eyes with 3 day chronic IOP elevation, only 1 explant had moving mitochondria. While there were occasional control explants with minimal movement, the

lack of motion in this group was dramatic. In the one chronic IOP explant with mitochondrial motion, the distance, speed, and percentage in motion were similar to control explants at 1 minute after imaging commenced (Table 6). However, by 10 minutes into imaging, <1% were moving anterograde (compared to >5% initially) and none was observed moving retrograde. Additionally, the mobile mitochondria in the 3 day glaucoma explants were moving 30% faster than matched controls at both baseline and 10 minutes.

In the control explants that underwent acute IOP increase, there was a significant increase in average distance traveled by mitochondria that were moving in the anterograde direction after IOP was 30 mmHg for 60 minutes ($p= 0.02$, t-test, pooled data for all eyes). The general trend for the pooled data also suggested that the speed of movement and number moving had decreased after 60 minutes at 30 mm Hg in the anterograde data (Figure 5C). We next calculated the change from baseline IOP to 30 mm Hg at 1 minute and 1 hour for each specimen. In the anterograde direction, there was a 63% increase in percent of mitochondria in motion when comparing 10mmHg (baseline) to 30 mmHg for 1 minute. Then, there was a 55% decrease from baseline in anterograde mitochondria in motion after 1 hour at 30 mm Hg ($p = 0.03$, paired t test). Percent of mitochondria that were moving also fell in the retrograde direction by 1 hour at 30 mm Hg, but this was not statistically significant (34% decrease, $p = 0.2$). The paired data within specimens showed a decrease in speed of 12-13% both anterograde and retrograde ($p = 0.3, 0.4$).

4. Discussion

A major drawback of past glaucoma research on RGC axons and ONH astrocytes has been the inability to study neurons and glia *in situ* in living tissue. Our new explant model utilizes methods by which fundamental changes in axons can be quantitatively measured, using laser scanning images of the ONH and retrobulbar optic nerve, the site of initial glaucoma damage. Previous models, including dissociated RGC (Welsbie et al., 2013), retinal explant cultures (Bull et al., 2011; Johnson et al., 2016) and eye cup models (Ishikawa et al., 2014), have been reported in which RGC survive for 1-2 weeks without a blood supply, despite transected axons, allowing repeated measures of RGCs over time. These each have advantages, but none preserves the actual tissue relationships of RGC axons in the ONH, and none permits manipulation of IOP in the intact globe to determine its effect in real time on the axons and astrocytes. Additionally, this new explant model allows for imaging with higher resolution than previously seen. Koch et al. (2015) imaged orbital optic nerve in anesthetized rats, showing axon effects after crush. However, rats have not yet been reengineered to have internal fluorescent markers in optic nerve neuronal components. Mouse retinal nerve fiber layer is visible through the sclera with confocal ophthalmoscopy (Takihara et al., 2015), allowing the measurement of mitochondrial movement with selectively fluorescent mitochondria. However, the critical early site of axonal injury in glaucoma, the ONH (Quigley et al., 1981), is only visible with our method, which permits quantification of individual fluorescent mitochondrial axonal transport speed and density in the ONH and retrobulbar nerve at higher resolution. Through use of controlled acute IOP elevation and prior chronic IOP exposure and pharmacological treatment, we can view the earliest changes of experimental glaucoma in real time and perform studies that detect beneficial therapeutic directions.

Our study has shown that fluorescent axons and mitochondria retain normal structure and function for 3-4 hours under confocal imaging in the explant model, as would have been expected from past retinal explant work. The neuronal cell body and its attached axon in cultured neurons have been shown in other models to have stable axonal transport for 6-12 hours, despite separation from their blood supply. It is probable that the mitochondria within axons provide the needed energy for some hours. This is by comparison to models in which dissociated RGCs or retinal explants have been subjected to ambient pressures above atmospheric levels on the cell soma, which does not mimic the local detrimental mechanical effects of IOP elevation at the ONH on RGC axons through stress from the peripapillary sclera and from the translaminar pressure differential. As previously suggested (Minckler et al., 1978) and as demonstrated here, the mitochondrial total area is higher near to the ONH than more distally in control explants. This may result from a greater need for ATP-based energy in the axons at this site, which approaches the first myelinated segment of the axon (Bristow et al., 2002). Using the new model, local treatments can be applied and the effect of previous chronic glaucoma studied. Internal axonal and astrocytic structure is quantifiable and real time video is possible.

The speed and motion behavior in our study of axonally transported mitochondria is intriguing, in that they are very similar to measurements of these parameters in cultured neurons. These measurements are clearly easier to carry out in single neurons on a flat culture dish where the movement of the preparation is highly controllable. We have been able to monitor the speed of movement of large numbers of mitochondria and find that over 80-90% are stationary at a given period of time—as has been demonstrated in cultured neurons. Also, as previously reported, there is a greater proportion of mitochondria moving in the anterograde direction than retrograde. Also, the movement in past reports was faster retrograde than anterograde (Misgeld et al., 2007), as our explants show. In control explants, anterogradely moving mitochondria were more frequent than retrograde ones, and moved longer distances but at a slower pace than the retrograde ones. We can speculate that since anterograde mitochondria have higher levels of ATP, the slower pace may make up for their lower speed—potentiating their ability to deliver ATP to the axon. By the same argument, retrogradely moving mitochondria would benefit from more rapid speeds to return to the soma to recharge.

Initial studies in this explant model clearly show that acute elevations of IOP result in changes to RGC mitochondrial behavior, illustrated here by studies of the distribution, size and speed of axonal transport among mitochondria. With acute IOP increase to 30 mm Hg for 3-4 hours, mitochondrial total area and mean diameter both decreased, compared to their baseline values, yet the density (number of mitochondria per unit area) was relatively unchanged. In explanted nerves, the mean mitochondrial size was reduced by up to 13% after 3-4 hours of IOP increase. This suggests that mitochondria have undergone fission with IOP-induced stress. The size of mitochondria is normally controlled by the process of joining and dividing (fusion and fission) which occur in response to tissue conditions. In past reports using cultured neurons, mitochondria responded with fission to increased hydrostatic pressure (Ju et al., 2007). Furthermore, the fission of mitochondria in the DBA/2J mouse model of glaucoma has also been reported (Coughlin et al., 2015). We will

conduct further studies of this phenomenon to determine if this response is a beneficial, adaptive reaction or a pathological step toward axonopathy (Kim et al., 2015).

In addition to change in mitochondrial size, acute IOP elevation affected the number and rate of mitochondrial movement in axonal transport. Within one minute of acute IOP increase, the proportion of mitochondria moving anterograde increased by >60%, then rapidly decreased at one hour of IOP elevation to 55% of control values. Similar, but smaller decreases in the proportion of mitochondria moving retrograde occurred. There was a trend toward slower speed of movement as well. Reduction in mitochondrial speed of movement was detected after laser injury of single cultured RGCs (Yokota et al., 2015). Again, it is not clear whether the fact that mitochondria decreased in their motion is a sign of injury or a potentially beneficial response to the stress of IOP elevation. Further study is indicated to answer this question.

In chronic mouse glaucoma models, axonal abnormality by past histological methods (Howell et al., 2007) was first detected as axon swelling by accumulation of vesicles and mitochondria. It was presumed that this resulted from axonal transport obstruction. Our findings in the RGC-YFP explants demonstrate that by 14 hours after IOP elevation, averaging about 30 mm Hg, axons are swollen and fragmented in the ONH and immediately retrobulbar nerve of the mouse. This axonal degeneration was progressively worse from 1 day to 1 week after chronic IOP elevation. We believe that these are the first images of actively dying RGC in experimental glaucoma. The magnitude of axon integrity loss measured here was similar to that in crushed, living rat RGC axons (Koch et al., 2015). The parallel finding of clumped mitochondria in axons of the ONH region within days after IOP elevation indicates that axonal transport disruption accompanies this axonal fragmentation. Indeed, the quantified mitochondrial density increased after 3 days of IOP elevation. Furthermore, in contrast to the acute IOP elevation studies, the total area of mitochondria also increased with 3 days of IOP elevation, while the mean size per mitochondrion was similar to control. Thus, the data after extended IOP elevation show a dominant effect of accumulation of mitochondria, while the apparent fission seen acutely is either no longer present, or is not as easily detected with the substantial clumping in the chronic specimens. After chronic IOP elevation as short as 3 days, mitochondrial movement was not evident in 3 of 4 explants and rapidly deteriorated over 10 minutes in one specimen (compared to continued movement in controls). In the 3 day glaucoma tissue, the proportion of mitochondria moving in anterograde direction changed from a total of >5% mobile to less than 1% over 10 minutes. Clearly, it will be useful to study the alterations occurring in the first days after IOP elevation, which precede both axon and RGC body death, in order to determine key pathways in cell injury.

We have developed a similar explant model to study the biomechanical behavior of the astrocytic lamina cribrosa and peripapillary sclera of the mouse eye (unpublished results, Cathy Nguyen) under controlled, living conditions. Like the model reported here, the eye is rapidly removed and kept in a moist environment. To view the behavior of the cellular lamina cribrosa of the mouse, however, we remove the entire optic nerve up to the sclera and view the astrocytes comprising the mouse lamina perpendicular to the lamina. We have used this explant model to study several genetically modified mouse lines with fluorescent axons,

mitochondria, or astrocytes. The stress—strain behavior of the mouse astrocytic lamina has been quantified by controlled IOP change in the explant. Prior treatment of the mouse during life with elevated IOP has shown changes in the physiological behavior of the lamina and peripapillary sclera in the mouse tissue that are likely to represent what occurs in its living state. Initial studies in this second explant model in normal eyes and after acute and chronic elevated IOP have provided stress—strain data relevant to glaucoma pathogenesis and suggesting potential neuroprotective approaches that can be tested in living animals.

The present model has some limitations. The imaging cannot be performed through the entire optic nerve thickness, though we estimate that data are obtained from over half of the nerve diameter. In some control specimens, mitochondria are no longer moving, perhaps due to damage during explant preparation. While both structure and mitochondrial parameters were generally stable during 3-4 hours *ex vivo*, we detected an increase in speed of movement during the first 10 minutes in the imaging setting. This may indicate that baseline measurements must be equilibrated for a short period. The manual method of following movement in sequential images would benefit from an automated kymographic approach, but none that has been previously described could be successfully implemented in these explant data.

In summary, we describe an explant model that offers detailed measurements of axonal behavior at the mouse ONH under controlled IOP conditions. The axons appear to retain normal functions within the limits reported here. The behaviors follow known features of axon degeneration and mitochondrial behavior as reported in histological studies and research with cultured neurons, but with retention of the normal tissue relationships of the ONH. Axonal fragmentation and change in mitochondrial transport have been detected within hours of acute or chronic IOP increase. These experiments can be potentially used to derive therapeutic directions to protect RGCs from loss of normal axonal and mitochondrial function.

Acknowledgments

This work was supported in part by PHS research grants EY 02120 and EY 01765 (Dr Quigley, and Wilmer Institute Core grant), and by unrestricted support from Saranne and Livingston Kosberg and from William T. Forrester. The funders had no role in study design, data collection and analysis, decision to publish, or preparation of the manuscript.

References

Anderson DR, Hendrickson A. Effect of intraocular pressure on rapid axoplasmic transport in monkey optic nerve. Invest Ophthalmol. 1974; 13:771–783. [PubMed: 4137635]

Barron MJ, Griffiths P, Turnbull DM, Bates D, Nichols P. The distributions of mitochondria and sodium channels reflect the specific energy requirements and conduction properties of the human optic nerve head. Br J Ophthalmol. 88:2004. 286–290.

Bristow EA, Griffiths PG, Andrews RM, Johnson MA, Turnbull DM. The distribution of mitochondrial activity in relation to optic nerve structure. Arch Ophthalmol. 2002; 120:791–796. [PubMed: 12049585]

Bull ND, Johnson TV, Welsapar G, DeKorver NW, Tomarev SI, Martin KR. Use of an adult rat retinal explant model for screening of potential retinal ganglion cell neuroprotective therapies. Invest Ophthalmol Vis Sci. 2011; 52:3309–3320. [PubMed: 21345987]

Coughlin L, Morrison RS, Horner PJ, Inman DM. Mitochondrial morphology differences and mitophagy deficit in murine glaucomatous optic nerve. Invest Ophthalmol Vis Sci. 2015; 56:1437–46. [PubMed: 25655803]

Dai Y, Weinreb RN, Kim KY, Nguyen D, Park S, Sun X, Lindsey JD, Ellisman MH, Ju WK. Inducible nitric oxide synthase-mediated alteration of mitochondrial OPA1 expression in ocular hypertensive rats. Invest Ophthalmol Vis Sci. 2011; 52:2468–76. [PubMed: 21220562]

Howell GR, Libby RT, Jakobs TC, Smith RS, Phalan FC, Barter JW, Barbay JM, Danaf RN, Huberman AD. Characteristic Patterns of Dendritic Remodeling in Early-Stage Glaucoma: Evidence from Genetically Identified Retinal Ganglion Cell Types. J Neurosci. 2015; 35:2329–2343. [PubMed: 25673829]

Inman DM, Lambert WS, Calkins DJ, Horner PJ. a-Lipoic Acid Antioxidant Treatment Limits Glaucoma-Related Retinal Ganglion Cell Death and Dysfunction. PLoS ONE. 2013; 8:e65389. [PubMed: 23755225]

Ishikawa M, Yoshitomi T, Zorumski CF, Izumi Y. Neurosteroids are endogenous neuroprotectants in an ex vivo glaucoma model. Invest Ophthalmol Vis Sci. 2014; 55:8531–8541. [PubMed: 25406290]

Johnson TV, Oglesby EN, Steinhart MR, Cone-Kimball E, Jeffreys J, Quigley HA. Time-Lapse Retinal Ganglion Cell Dendritic Field Degeneration Imaged in Organotypic Retinal Explant Culture. Invest Ophthalmol Vis Sci. 2016; 57:253–264. [PubMed: 26811145]

Ju WK, Liu Q, Kim KY, Crowston JG, Lindsey JD, Agarwal N, Ellisman MH, Perkins GA, Weinreb RN. Elevated hydrostatic pressure triggers mitochondrial fission and decreases cellular ATP in differentiated RGC-5 cells. Invest Ophthalmol Vis Sci. 2007; 48:2145–2151. [PubMed: 17460273]

Kalesnykas G, Oglesby EN, Zack DJ, Cone FE, Steinhart MR, Tian J, Pease ME, Quigley HA. Retinal ganglion cell morphology after optic nerve crush and experimental glaucoma. Invest Ophthalmol Vis Sci. 2012; 53:3847–3857. [PubMed: 22589442]

Kang JS, Tian JH, Pan PY, Zald P, Li C, Deng C, Sheng ZH. Docking of axonal mitochondria by syntaphilin controls their mobility and affects short-term facilitation. Cell. 2008; 132:137–148. [PubMed: 18191227]

Kim KY, Perkins GA, Shim MS, Bushong E, Alcasid N, Ju S, Ellisman MH, Weinreb RN, Ju WK. DRP1 inhibition rescues retinal ganglion cells and their axons by preserving mitochondrial integrity in a mouse model of glaucoma. Cell Death Dis. 2015; 6:e1839. [PubMed: 26247724]

Knöferle J, Koch J, Ostendorf J, Michel U, Planchamp V, Vutova P, Tönges L, Stadelmann C, Brück W, Bähr M, Lingora P. Mechanisms of acute axonal degeneration in the optic nerve in vivo. Proc Natl Acad Sci. 2010; 107:6064–6069. [PubMed: 20231460]

Koch JC, Bitow F, Haack J, d'Hedouville Z, Zhang JN, Tönges L, Michel U, Oliveita LM, Jovin TM, Liman J, Tatenhorst L, Bähr M, Lingor P. Alpha-synuclein affects neurite morphology, autophagy, vesicle transport and axonal degeneration in CNS neurons. Cell Death Dis. 2015; 6:1811.

Lee D, Shim MS, Kim KY, Noh YH, Kim H, Kim SY, Weinreb RN, Ju WK. Coenzyme Q10 inhibits glutamate excitotoxicity and oxidative stress-mediated mitochondrial alteration in a mouse model of glaucoma. Invest Ophthalmol Vis Sci. 2014; 55:993–1005. [PubMed: 24458150]

Loverde JR, Ozoka VC, Aquino R, Lin L, Pfister BJ. Live imaging of axon stretch growth in embryonic and adult neurons. J Neurotrauma. 2011; 28:2389–2403. [PubMed: 21663384]

Leung CK, Weinreb RN, Li ZW, Liu S, Lindsey JD, Choi N, Liu L, Cheung CY, Ye C, Qiu K, Chen LJ, Yung WH, Crowston JG, Pu M, So KF, Pang CP, Lam DS. Long-term in vivo imaging and measurement of dendritic shrinkage of retinal ganglion cells. Invest Ophthalmol Vis Sci. 2011; 52:1539–1547. [PubMed: 21245394]

Marchant JK, Mahesh N, Prociatti V, Whitemore AV, Masland RH, John SW. Axons of retinal ganglion cells are insulted in the optic nerve early DBA/2J glaucoma. J Cell Biol. 2007; 179:1523–1537. [PubMed: 18158332]

McElnea EM, Quill B, Docherty NG, Irnaten M, Siah WF, Clark AF, O'Brien CJ, Wallace DM. Oxidative stress, mitochondrial dysfunction and calcium overload in human lamina cribrosa cells from glaucoma donors. Mol Vis. 2011; 17:1182–91. [PubMed: 21617752]

Miller KE, Sheetz M. Axonal mitochondrial transport and potential are correlated. J Cell Sci. 117:2004. 2791–2804.

Miller KE, Sheetz M. Direct evidence for coherent low velocity axonal transport of mitochondria. J Cell Biol. 173:2006. 373–381.

Minckler DS, Bunt AH, Klock IB. Radiographic and cytochemical ultrastructural studies of axoplasmic transport in the monkey optic nerve head. Invest Ophthalmol Vis Sci. 1978; 17:33–50. [PubMed: 74368]

Misgeld T, Kerschensteiner M, Bareyre FM, Burgess RW, Lichtman JW. Imaging axonal transport of mitochondria in vivo. Nature Methods. 2007; 4:559–561. [PubMed: 17558414]

Osborne NN. Mitochondria: Their role in ganglion cell death and survival in primary open angle glaucoma. Exp Eye Res. 2010; 90:750–757. [PubMed: 20359479]

Quigley HA, Addicks EM, Green WR, Maumenee AE. Optic nerve damage in human glaucoma. II. The site of injury and susceptibility to damage. Arch Ophthalmol. 1981; 99:635–649. [PubMed: 6164357]

Quigley HA, Broman A. The number of persons with glaucoma worldwide in 2010 and 2020. Br J Ophthalmol. 2006; 90:151–156.

Sheng ZH, Cai Q. Mitochondrial transport in neurons: impact on synaptic homeostasis and neurodegeneration. Nature Reviews Neurosci. 2012; 13:77–93.

Takihara Y, Inatania M, Etoc K, Inoue T, Kreymerman A, Miyake S, Ueno S, Nagaya M, Nakanishi A, Iwao K, Takamura Y, Sakamoto H, Satho K, Kondo M, Sakamoto T, Goldberg JL, Nabekura J, Tanihara H. In vivo imaging of axonal transport of mitochondria in the diseased and aged mammalian CNS. Proc Natl Acad Sci. 2015; 18:10515–10520.

Tezel G. The immune response in glaucoma: a perspective on the roles of oxidative stress. Exp Eye Res. 2011; 93:178–86. [PubMed: 20709058]

Welsbie D, Yang Z, Yan Z, Ge Y, Mitchell KL, Zhou X, Martin SE, Berlinkicke CA, Hackler L Jr, Fuller J, Cao LH, Han B, Auld D, Xue T, Hirai S, Germain L, Simard- Bosson C, Blouin R, Nguyen JV, Davis CH, Enke RA, Boye SL, Merbs SL, Marsh-Armstrong N, Hauswirth WW, DiAntonio A, Nickells RW, Inglese J, Hanes J, Yau KW, Quigley HA, Zack DJ. Functional genomic screening identifies dual leucine zipper kinase as a key mediator of retinal ganglion cell death. Proc Natl Acad Sci. 2013; 110:4045–4050. [PubMed: 23431148]

Yokota S, Takihara Y, Arimura S, Miyake S, Takamura Y, Yoshimura N, Inatani M. Altered transport velocity of axonal mitochondria in retinal ganglion cells after laser-induced axonal injury in vitro. Invest Ophthalmol Vis Sci. 2015; 56:8019–8025. [PubMed: 26720449]

Abbreviations

ONH	Optic Nerve Head
ON	Optic Nerve
IOP	Intraocular pressure
YFP	Yellow Fluorescent Protein
CFP	Cyan Fluorescent Protein
ATP	Adenosine Triphosphate
RGC	Retinal ganglion cell
RGC-YFP	Mouse strain expressing YFP in selected axons
Mito-CFP	Mouse strain expressing CFP in all mitochondria
Thy1	Thymus cell antigen 1, theta promoter
NB	Neurobasal Solution

LSM 710 Zeiss 710 Confocal Laser Scanning Microscope

Highlights

- An explant model of the mouse eye was developed to facilitate the study of retinal ganglion cell axons and mitochondria in the living optic nerve head, the site of glaucoma injury
- Using laser scanning microscopy imaging was possible and stable (for 3 hours) in two transgenic mouse strains; one expressing fluorescent protein in selected retinal ganglion cell axons and another expressing all mitochondria.
- Glaucoma bead model caused a significant increase in mitochondria density, a decrease in mitochondrial length, and decrease in mitochondrial movement.
- Glaucoma also caused fragmentation of axon structures at the ONH, increasing in severity with longer periods of glaucoma exposure.

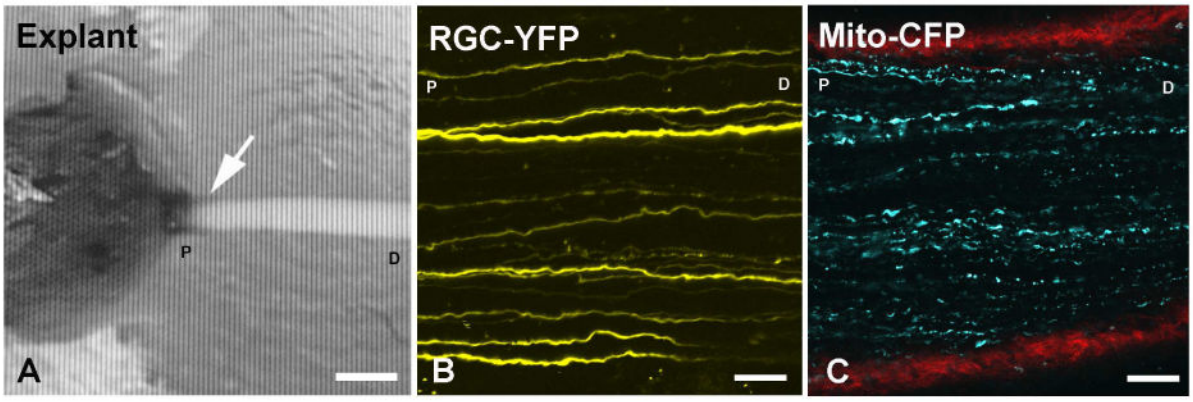

Figure 1.

(A) Explant of eye and optic nerve fixed to a plastic block with agarose covering the tissue (arrow = the optic nerve head region, bar = 400 μm). Imaging of the optic nerve is performed perpendicular to nerve along axis. The attached optic nerve is ~3 mm long. (B) Confocal image of RGC-YFP explant with selectively YFP-expressing axons. (C) Mito-CFP explant showing mitochondria (blue) and collagen in red (second harmonic generation imaging). Labels: D- distal to the eye, P-proximal to the eye (at the ONH) are used to indicate orientation (B, C: bars = 25 μm).

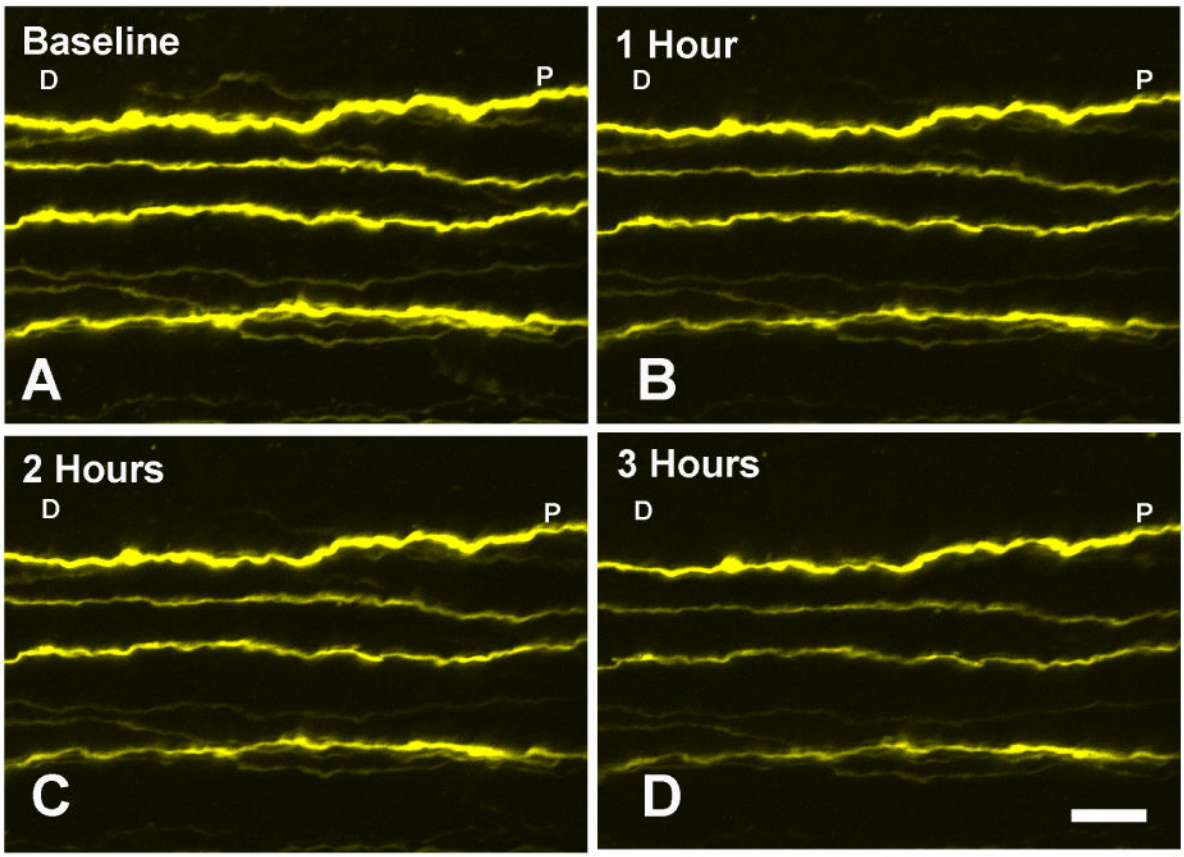

Figure 2.

One RGC-YFP control explant imaged at 4 time points; (A) baseline, (B) 1 hour, (C) 2 hours, and (D) 3 hours from start of imaging shows selectively fluorescent axon structure stability. Appearance changes minimally from baseline IOP of 10 mm Hg. Labels: D- distal to the eye, P-proximal to the eye (at the ONH) are used to indicate orientation (bar = 10 μm).

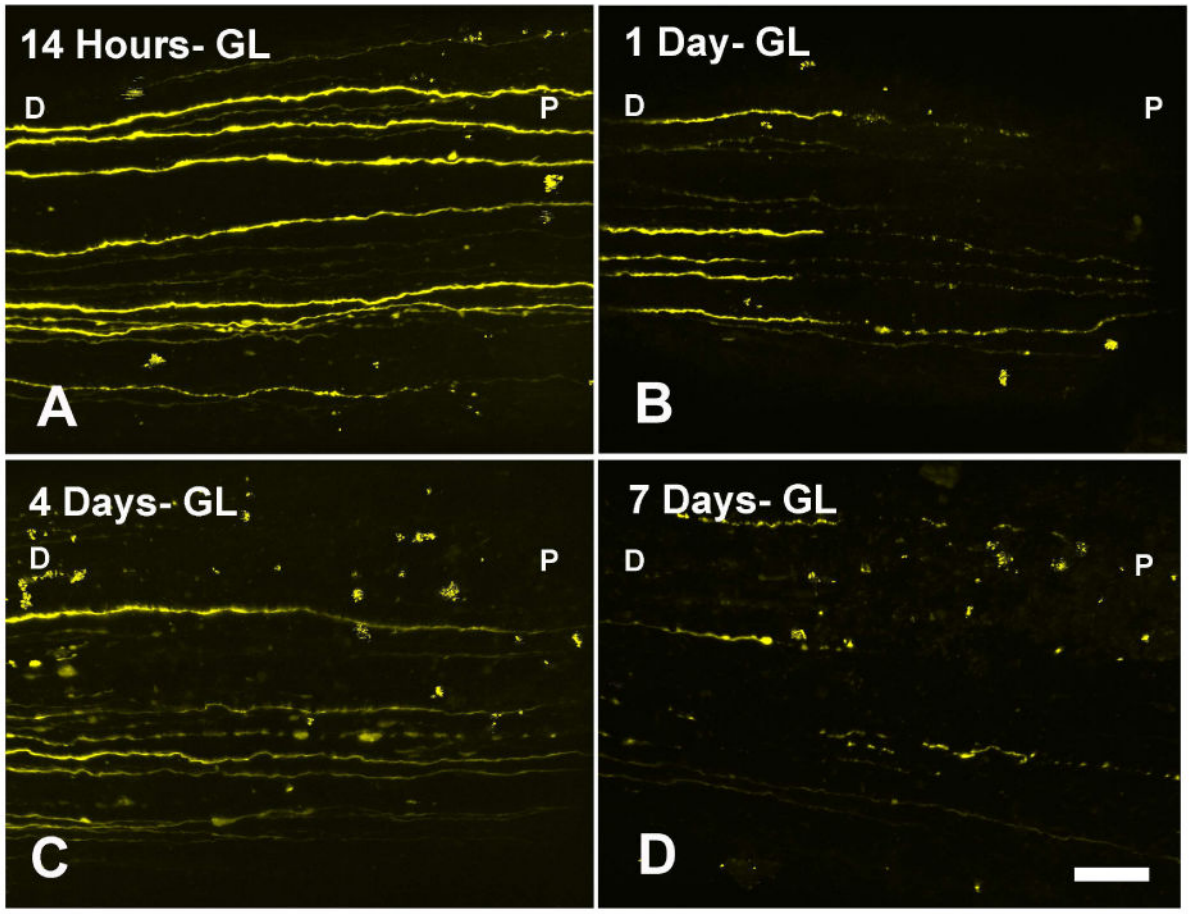

Figure 3.

RGC-YFP axons show progressive fragmenation, swelling, and loss after IOP elevation in the bead-induced model at (A) 14 hours, (B) 1 day, (C) 4 days, and (D) 1 week post chronic IOP elevation. Labels: D-distal to the eye, P-proximal to the eye (at the ONH) are used to indicate orientation (bar = 30 μm).

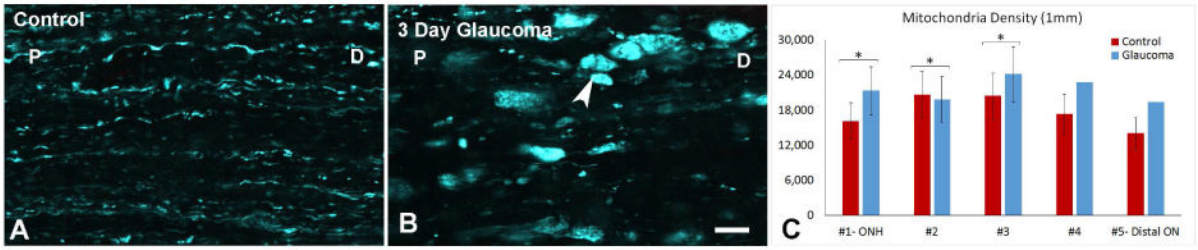

Figure 4.

Mitochondrial Density. (A) Mitochondria in control explant. (B) Three day glaucoma explant showing mitochondrial transport block with clumping. Labels: D- distal to the eye, P-proximal to the eye (at the ONH) are used to indicate orientation (arrow head; bar = 10 μm). (C) Mitochondrial density (percent area occupied by mitochondria) in serial zones from ONH to 1 mm behind eye, showing significantly increased density after chronic IOP elevation (* = $p < 0.05$, locations #4 and #5 have no error bars due to limited sample size).

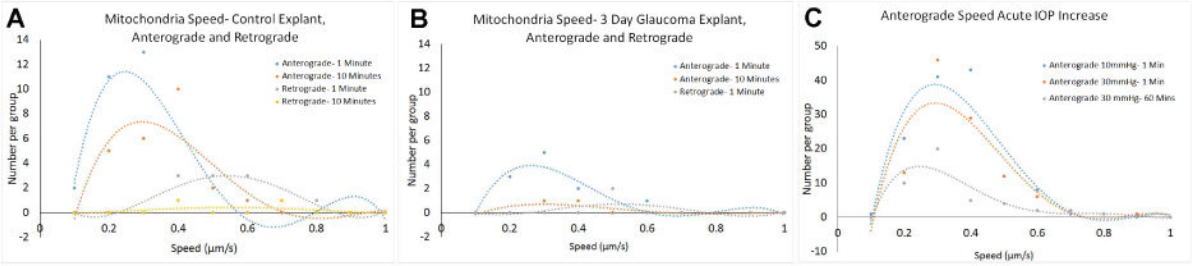

Figure 5.

Anterograde and retrograde speed and number of mitochondria in motion in (A) Control explants and (B) 3 day chronic glaucoma explants (1 and 10 minutes after initiation of imaging). (C) Anterograde speed after acute IOP elevation from 10 mm Hg to 30mm Hg for 1 minute and 60 minutes (curves represent polynomial fits to data).

Table 1

Number of eyes and mice studied of each type in various protocols.

Strain	Study	Time Points	Eyes (Animals)
RGC-YFP	Axon stability	Control	N= (1)
RGC-YFP	Axon Integrity (Acute IOP Elevation)	3 Hours	N= (5)
RGC-YFP	Axon Integrity (Chronic IOP Elevation)	Control 14 hours 1 Day 4 Days 7 Days	N=3 N=6 N=5 N=7 N=7 Total = 28 (25)
Mito-CFP	Stability Imaging (Density and Size)	Control	N=4 (2)
Mito-CFP	Mitochondrial Density and Size (Acute IOP Elevation)	3 Hours 4 Hours	N=11 N=10 Total= 21 (11)
Mito-CFP	Mitochondrial Density and Size (Chronic IOP Elevation)	Control 3 Day Glaucoma	N=14 N=8 Total = 22 (20)

Table 2

Axonal integrity measurements in RGC-YFP explant tissue after chronic IOP elevation (GL).

Group	# Eyes	IOP at Sacrifice	# Nerves	# Axons Counted	Median # Fragments (per Axon)	Median Fragment Length	Mean Fragment Total Length	Mean Axon Length	Median Integrity Ratio
Control	3	12	3	23	1	353	388 ± 38	393 ± 38	1.00
14 hour GL	6	28	6	77	8.0	35	318 ± 108	395 ± 55	0.81
1 Day GL	4	28	5	29	6.0	34	341 ± 147	375 ± 81	0.77
4 Day GL	7	26	7	34	6.5	21	215 ± 139	379 ± 91	0.52
7 Day GL	7	18	7	47	7.0	26	229 ± 142	410 ± 41	0.49

Table 3

Mitochondria Count, Diameter, Area and Density in control explants

CONTROL	#1- ONH	#2	#3	#4	#5- Distal ON
Mitochondria Count	322	412	408	347	280
Mean Diameter ± StDev (μm)	1.5 ± 1.1	1.3 ± 1.1**	1.3 ± 1.0**	1.1 ± 0.8*	1.2 ± 0.9*
Total Area (μm^2)	757	774	689	430	411
Density (mitochondria/mm^2)	16,110 ± 3,159	20,600 ± 4,039*	20,400 ± 4,000*	17,342 ± 3,400	14,010 ± 2,747
N	10	9	9	6	5
% Decrease from Total area #1		-2.3%**	9%**	43%**	46%**

Total Area= Area of all mitochondria with image window

Density= number of mitochondria in window (200μm × 100 μm)

For Diameter and Decrease from Total area, p-values compare location # 1 proximal to the eye (ONH) to distal locations along the nerve:

* = p ≤ 0.05, and

** = p ≤0.01.

Mean ± standard deviation

Table 4

Mitochondria Count, Diameter, Area and Density in Chronic IOP Elevation Explants

3 Day GLAUCOMA	#1- ONH	#2	#3	#4	#5- Distal ON
Mitochondria Count	400	495	604	569	485
Mean Diameter ± StDev (μm)	1.4 ± 1.1	1.3 ± 1.3	1.3 ± 1.0	1.0 ± 0.7	1.1 ± 0.7
Total Area (μm^2)	903	1006	1148	745	675
Density (mitochondria/mm^2)	21,300 ± 4,176 *	19,800 ± 3,882 **	24,170 ± 4,739 **	22,760	19,400
N	4	4	4	1	1
% Increase in Total Area: Glaucoma compared to control	19%	30%	67% **	73%	64%

Total Area= Area of all mitochondria with image window

Density= number of mitochondria in window (200μm × 100 μm)

For Density data, p-values compare glaucoma tissue to corresponding control tissue locations.

For % Increase in Total Area, p-values compare glaucoma to control at same distance from nerve (

* = $p \leq 0.05$, and

** = $p \leq 0.01$).

Mean ± standard deviation

Table 5

Acute IOP Elevation: Mitochondrial Total Area and Diameter

Acute IOP Elevation	10mmHg-1Min	30mmHg-1Min	30mmHg- 1 Hr	30mmHg-2 Hr	30mmHg- 3 Hr	30mmHg- 4Hr	10mmHg-10Min
Mitochondria Count	236	224	237	231	233	232	237
Mean Diameter ± StDev (μm)	2.3 ± 1.4	2.3 ± 1.3	2.2 ± 1.4	2.2 ± 1.4	2.0 ± 1.2	2.0 ± 1.2	2.0 ± 1.2
Total Area (μm^2)	972	888	917	900	823	791	839
Density (mitochondria/mm^2)	12,602 ± 4127	11,317 ± 2430	12,417 ± 3877	12,152 ± 3579	12,570 ± 3892	11,623 ± 2874	12,092 ± 3660
N	21	18	21	21	22	11	18
% Diameter Decrease		1%	3%	5%	11%	13%	11%
% Diameter Decrease p-value		0.83	0.54	0.16	0.005	0.015	0.006

Mean ± standard deviation

Table 6

Mitochondrial % moving, distance moved, and speed in anterograde and retrograde direction for control, 3 day chronic, and Acute IOP elevation explants. Count = average number of mitochondria in imaging window (200μm × 100 μm). Mean ± standard deviation.

	Anterograde					Retrograde				
Experimental Groups	**Samples (Movement Measured)**	**Mitochondria Count**	**Mitos Moving (%)**	**Distance (μm)**	**Speed (μm/s)**	**Samples (Movement Measured)**	**Mitochondria Count**	**Mitos Moving (%)**	**Distance (μm)**	**Speed (μm/s)**
Control-1 Minute	4 (3)	302	3.42 ± 1.69	11.30 ± 2.91	0.22 ± 0.10	4 (3)	302	1.09 ± 0.70	10.63 ± 2.37	0.50 ± 0.12
Control-10 Minutes	4 (3)	302	2.42 ± 1.82	12.92 ± 4.86	0.30 ± 0.11	4 (3)	302	0.44 ± 0.10	10.31 ± 3.48	0.79 ± 0.33
Glaucoma-1 Minute	4 (1)	214	5.14	13.64 ± 5.32	0.27 ± 0.11	4 (1)	214	0.93	11.03 ± 0.49	0.46 ± 0.02
Glaucoma-10 Minutes	4 (1)	214	0.93	12.10 ± 4.26	0.31 ± 0.04	4 (0)	214			
Acute IOP: 10 mm Hg- 1 Minute	21 (10)	251	5.4 ± 4.48	13.18 ± 5.02	0.31 ± 0.13	21 (6)	237	1.76 ± 2.00	11.81 ± 3.35	0.34 ± 0.16
Acute IOP: 30 mmHg- 1 Minute	21 (8)	221	6.72 ± 4.00	13.21 ± 5.21	0.32 ± 0.13	21 (5)	206	1.22 ± 0.97	11.08 ± 4.17	0.29 ± 0.11
Acute IOP: 30 mmHg- 60 Minutes	21 (4)	222	5.35 ± 6.17	15.29 ± 5.95	0.30 ± 0.15	21 (4)	202	1.62 ± 1.04	12.95 ± 4.49	0.31 ± 0.13